

Provided for non-commercial research and educational use only.
Not for reproduction or distribution or commercial use.



Volume 252, No. 22, 15 September 2006 ISSN 0169-4332

applied surface science

A journal devoted to applied physics
and chemistry of surfaces and interfaces

Editors

F.H.P.M. Habraken, Utrecht, The Netherlands
H. Kobayashi, Osaka, Japan
J.E. Rowe, Raleigh, NC, USA
H. Rudolph, Utrecht, The Netherlands

Volume 252, No. 22, pp. 7749–8028

15 September 2006

Available online at: www.sciencedirect.com
 ScienceDirect
<http://www.elsevier.com/locate/apausc>

This article was originally published in a journal published by Elsevier, and the attached copy is provided by Elsevier for the author's benefit and for the benefit of the author's institution, for non-commercial research and educational use including without limitation use in instruction at your institution, sending it to specific colleagues that you know, and providing a copy to your institution's administrator.

All other uses, reproduction and distribution, including without limitation commercial reprints, selling or licensing copies or access, or posting on open internet sites, your personal or institution's website or repository, are prohibited. For exceptions, permission may be sought for such use through Elsevier's permissions site at:

<http://www.elsevier.com/locate/permissionusematerial>

Structural investigation of thin tetracene films on flexible substrate by synchrotron X-ray diffraction

S. Milita^{a,*}, C. Santato^b, F. Cicoira^b

^a *Istituto per la Microelettronica e i Microsistemi (IMM), Consiglio Nazionale delle Ricerche (CNR), Via Gobetti 101, 40129 Bologna, Italy*

^b *Istituto per lo Studio dei Materiali Nanostrutturati (ISMN), Consiglio Nazionale delle Ricerche (CNR), Via Gobetti 101, 40129 Bologna, Italy*

Received 10 February 2006; received in revised form 10 April 2006; accepted 10 April 2006

Available online 5 June 2006

Abstract

Structural properties of tetracene thin films grown by vacuum sublimation on a flexible Mylar[®] substrate have been investigated by means of synchrotron X-ray diffraction. The films are polycrystalline and are made up of crystalline domains oriented with the (0 0 *l*) planes almost parallel to the substrate and completely misoriented around the surface normal. Two crystallographic phases (α and β thin film phases) have been identified. They differ for the d_{hkl} interplanar spacing, both larger than that of the bulk. As a comparison, results from tetracene films grown on SiO₂ have been reported to investigate the different charge transport properties of films grown on Mylar and on SiO₂ substrates.

© 2006 Elsevier B.V. All rights reserved.

Keywords: Tetracene; Thin films; Synchrotron X-ray diffraction; Flexible substrate

1. Introduction

Organic thin films are of interest as active layers in electronic and optoelectronic devices such as field-effect transistors (FETs) [1–4], light-emitting diodes (LEDs) [5,6] and photovoltaic cells [7]. The interest for organic (opto-) electronics stems from the possibility to develop low cost, large area and flexible devices [8]. Organic light-emitting (field effect) transistors (OLETs) are a new class of organic optoelectronic devices that integrate the transistor function with the light emission [9]. Recently OLETs based on tetracene films deposited on flexible Mylar[®] foils, acting at the same time as dielectric and substrate, have been reported [10]. The optoelectronic properties of devices on Mylar are similar to those observed on the commonly employed dielectric SiO₂ [11]. As an example, drain-source current and light emission present the same correlation as a function of the drain and the gate polarizations. However, the use of the different dielectrics determines relevant differences in the performance of the

devices. For instance for devices on Mylar the hole FET mobility is more than one order of magnitude lower than for devices on SiO₂ and, unlike the case of SiO₂, no significant dependence of the mobility on the deposition flux has been observed [12].

The investigation of the effect of the dielectric on the structure and the morphology of the active layer is mandatory to understand the physics of the device and to improve its performance. It has been demonstrated that, in organic film-based FETs, charge transport occurs within a thin layer close to the organic/dielectric interface [13].

Charge transport in organic semiconductors requires adequate overlap of the π orbitals on adjacent molecules that is provided by a good packing of the molecules [14]. This shows how crucial it is the role played by the structural characteristics of the active material in establishing charge transport properties [15,16].

In this work, we have performed a structural investigation of tetracene thin films deposited on Mylar and results have been compared with those obtained for tetracene films on SiO₂. We propose an explanation for the different charge transport properties in field-effect transistor configuration of tetracene thin films grown on Mylar and on SiO₂.

* Corresponding author. Tel.: +39 051 6399156; fax: +39 051 6399216.
E-mail address: milita@bo.imm.cnr.it (S. Milita).

2. Experimental

Tetracene films were deposited by vacuum sublimation on 900 nm thick Mylar foil (DuPont) adapted on Al frame [17]. The root mean square (rms) roughness of Mylar foil, measured by Atomic Force Microscopy was about 1 nm. The procedure to fix the foil to the support ensured a good flatness of the substrates, which is crucial for the structural features of the final films. With the aim of comparison, films were also deposited onto SiO₂ substrates, with a rms roughness of 0.2 nm. The experimental set up for film deposition has been detailed elsewhere [12]. Tetracene powder from Tokyo Chemical Industries was used as material source. Films with a nominal thickness of 50 nm were grown at deposition fluxes (F) of 0.01 and 0.5 nm/s.

X-ray diffraction measurements were performed at the XRD1 beamline of ELETTRA synchrotron facility (Trieste, Italy). A double crystal silicon monochromator was used to select the energy of 8.05 keV from the white emission spectrum of the wiggler source. The beam cross-section at the sample was limited by slits to 0.1 mm both in the horizontal and vertical directions.

Diffraction patterns in grazing incidence (GI) reflection and transmission geometries were recorded. In the former case, the monochromatic beam impinged on the sample with an incidence angle $\alpha_i \approx 1^\circ$. At this angle, the beam path in the film is strongly enhanced and its footprint on the surface (0.1 mm \times 6 mm) is fully included in the film. In the transmission geometry, the incoming beam was perpendicular to the backside of the surface sample. In both cases, a 2D CCD detector of 165 mm diameter was placed normal to the incident beam direction and 130 mm from the sample. The detector collected a wide range of scattering angles (up to 30° in our geometry), and simultaneously allowed the identification of the crystalline phases and the determination of the crystallite texturing.

3. Results and discussion

A 2D diffraction image was recorded in transmission mode from a glass capillary filled with tetracene powder (Fig. 1a) and was used as the reference standard for the diffraction of the thin films. Fig. 1b shows the 1D diffraction pattern (intensity integrated along the Debye rings versus scattering angle) extracted from the diffraction image. It was properly indexed by means of Powdercell software [18] using the crystallographic parameters and atom coordinates reported by Holmes et al. [19] for triclinic tetracene (space group $P\bar{1}$). The tetracene unit cell contains two planar molecules. The molecular planes are tilted with respect to one another in a herringbone structure and their long axes are parallel to each other and tilted by 22° from the normal to the (ab), or (001), plane.

Fig. 2a and b shows the reflection images of tetracene films deposited on Mylar at $F = 0.01$ and 0.5 nm/s. Each image is the overlapping of the diffractions from the film and the substrate, the scattering pattern of the latter being shown in Fig. 2c. The diffraction images of tetracene films deposited in the same

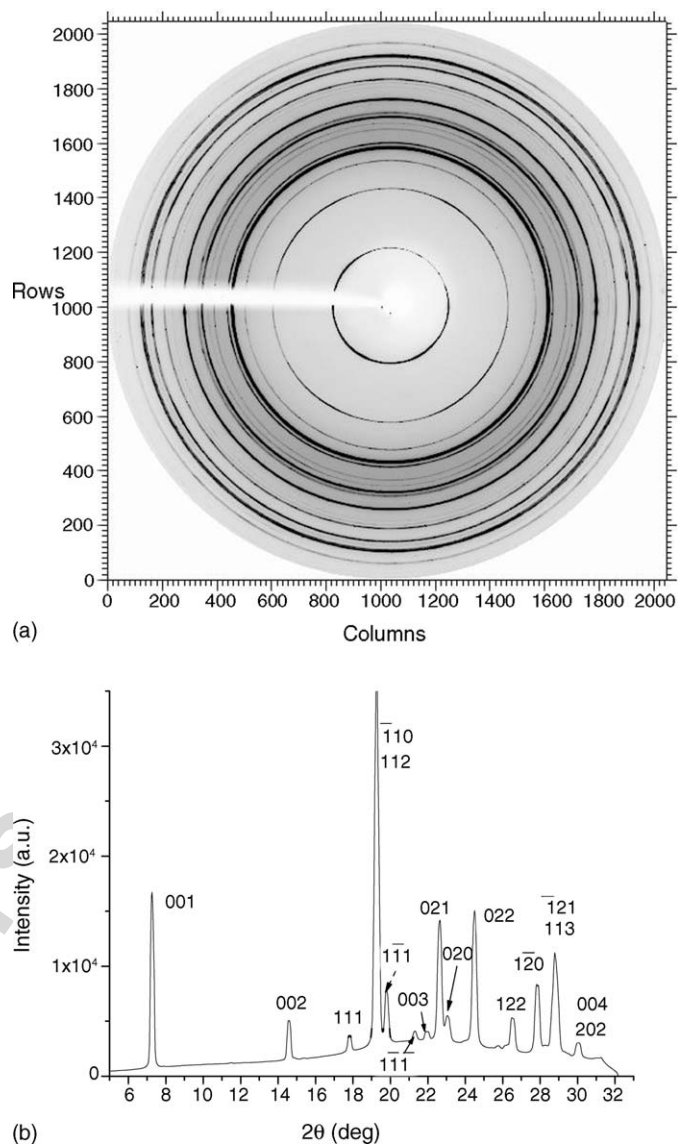


Fig. 1. Diffraction images of tetracene powder (a) and its integrated intensity over the Debye rings (b).

conditions on SiO₂, whose structural features have been already reported in [20], are shown for comparison in Fig. 2d and e. On both substrates tetracene films generate diffraction arcs and spots, indicating that they are formed by crystallites with a pronounced orientation. In the case of SiO₂, the increase in the deposition flux induces a strong increase in film texturing whereas no evidence in texturing evolution is observed for Mylar.

The fact that the 00 l reflections, unlike the hkl reflections, are concentrated on the central region of the 2D detector means that the crystalline domains are oriented with the (00 l) planes almost parallel to the substrate. The domains are completely misoriented around the surface normal (SN), as deduced by the invariance of the diffraction images recorded after sample rotation by any angle around its normal and by the symmetry of the hkl reflections with respect to the SN axis. Indeed, for a random distribution around the surface normal, each pair of the

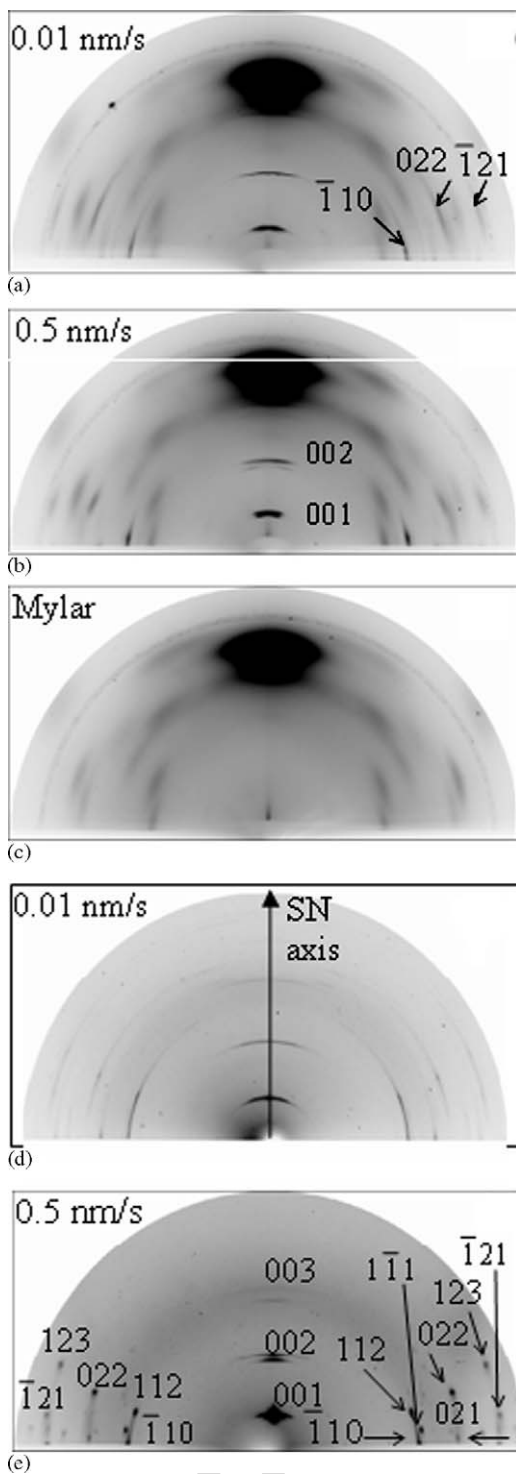


Fig. 2. Diffraction images recorded in grazing incidence (GI) reflection geometry of tetracene films grown at $F = 0.01$ and 0.5 nm/s, respectively, on Mylar (a and b) and on SiO_2 (d and e). The image diffracted by the pristine Mylar substrate is reported in (c). The surface normal (SN) axis is traced only in (d) for clarity. Nominal thickness of the films: 50 nm.

lateral spots corresponds to the two symmetric orientations at which the (hkl) planes are in the Bragg position. The azimuthal angle δ measured from the SN axis and the spots is a function of the angle between the diffracting plane and the surface, its Bragg angle and the incident angle of the X-ray beam [21].

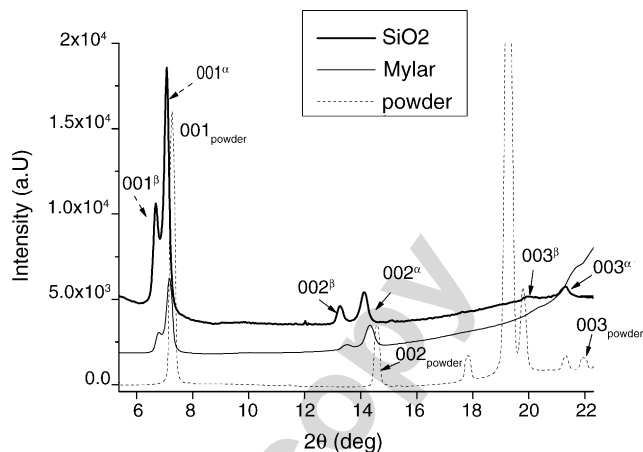


Fig. 3. Diffraction spectra of tetracene powder and of 50 nm-thick tetracene films deposited at $F = 0.5$ nm/s on Mylar and on SiO_2 . The intensity integration was performed over the Debye rings in the central region of the 2D detector.

The diffraction patterns of the tetracene powder and of the films deposited at $F = 0.5$ nm/s on Mylar and SiO_2 are compared in Fig. 3. For clarity, the intensity integration was done selectively over the central part of the 2D pattern diffracted from the film. On both substrates tetracene films show two peaks for each $00l$ reflection, which are shifted towards low scattering angles compared to those of the powder. This indicates the presence of two thin film phases, called α and β thin film phases in the following, which have d_{hkl} interplanar spacing larger than that of the bulk ($d_{00l,\beta} > d_{00l,\alpha} > d_{00l,\text{powder}}$). The d_{00l} distance goes from 1.213 ± 0.005 nm (powder) to 1.234 ± 0.005 nm in the α phase and to 1.359 ± 0.005 nm in the β phase. In both α and β thin film phases, the long molecular axis is nearly perpendicular to the substrate, as expected in the case of isotropic and inert substrates, where intermolecular interactions are stronger than substrate–molecule interactions [22].

The different lattice spacings of the two thin film phases indicate a different orientation of the tetracene molecules: in the more expanded β phase, the tilt angle of the molecular axis from the normal to the surface is smaller than in the α phase [23]. Fig. 4 shows the 001 peaks of tetracene films grown at the two fluxes on Mylar (a) and on SiO_2 (b). At $F = 0.01$ nm/s, i.e. in conditions close to the equilibrium, the α phase, which is thermodynamically more stable, is strongly dominant in both films (essentially the only one on SiO_2). At higher F , a large amount of the less stable β phase is observed on both substrates. This phase should be induced by a too fast nucleation and growth to allow relaxation to the more thermodynamically stable state.

In spite of the similarities between the structures of tetracene films grown on the two substrates, remarkable differences have been observed concerning the degree of crystallite misorientation and the atomic disorder of (hkl) planes.

The arc-shaped diffraction from the $(00l)$ planes indicates that they have an out-of-plane misorientation, μ_{out} , whose value is given by the angular widths of the arcs. The quite different azimuthal distributions of the $(00l)$ planes for the films on the two substrates indicate different preferential orientations, as reported for the α phase (which gives a diffracted signal more intense than that from the β phase) in Fig. 5. On Mylar (Fig. 5a) the

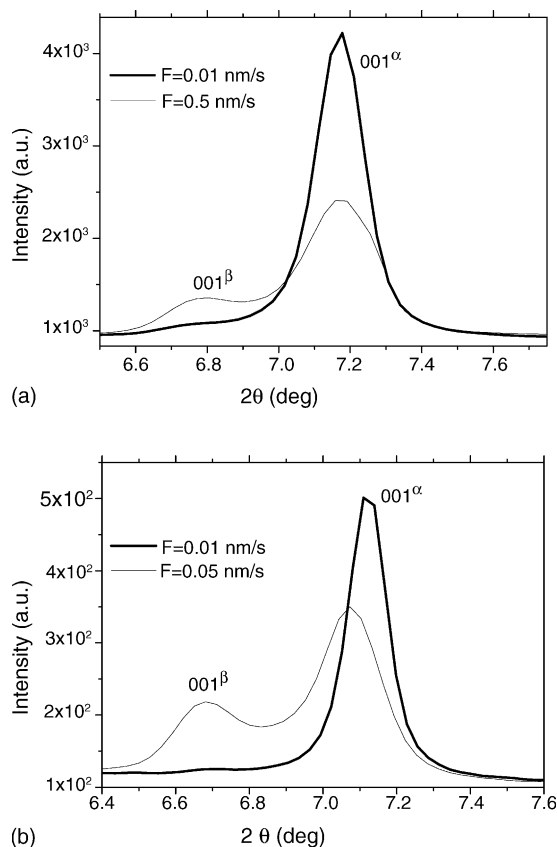


Fig. 4. 001 GI reflection profiles of 50 nm-thick tetracene films deposited at $F = 0.01$ and 0.5 nm/s on Mylar (a) and on SiO_2 (b). The intensity integration was performed over the Debye rings in the central region of the 2D detector.

diffracted signal is detected for a range of crystallite misorientation decreasing from $\mu_{\text{out}} = \pm 20^\circ$ to $\pm 16^\circ$ with increasing F from 0.01 to 0.5 nm/s. Moreover, at low F most of the crystallites have $\mu_{\text{out}} = \pm 6^\circ$, as evidenced by the presence of a double peak, whereas at higher F this type of preferential orientation almost disappears. On SiO_2 (Fig. 5b), regardless of F , most of the (001) planes lie preferentially parallel to the surface within $\mu_{\text{out}} = \pm 4^\circ$, and a smaller amount of crystallites is characterized by $\pm 12^\circ$. The other difference between tetracene films grown on the two substrates seems reasonably to deal with the atomic disorder in the (hkl) planes, as deduced by the following considerations. For tetracene films on SiO_2 (Fig. 2d and e), several hkl spots are recorded whereas only three hkl among the more intense reflections have been observed for films on Mylar (marked by arrows in Fig. 2a). This could result from a strong attenuation of their structure factors caused by static atomic disorder (Debye-Waller factor) in the (hkl) lattice planes. Since these planes are near normal to the surface, the atomic disorder in them should lower the π - π orbital overlapping with a strong impact on the charge transport properties in the films. These two structural differences are helpful for the understanding of the different charge transport properties of tetracene films on Mylar and on SiO_2 . The misorientation has a detrimental effect on the molecular packing that, leading to an extended electronic delocalization, is required for good charge transport. The atomic disorder decreases the π - π orbital overlapping thus leading to

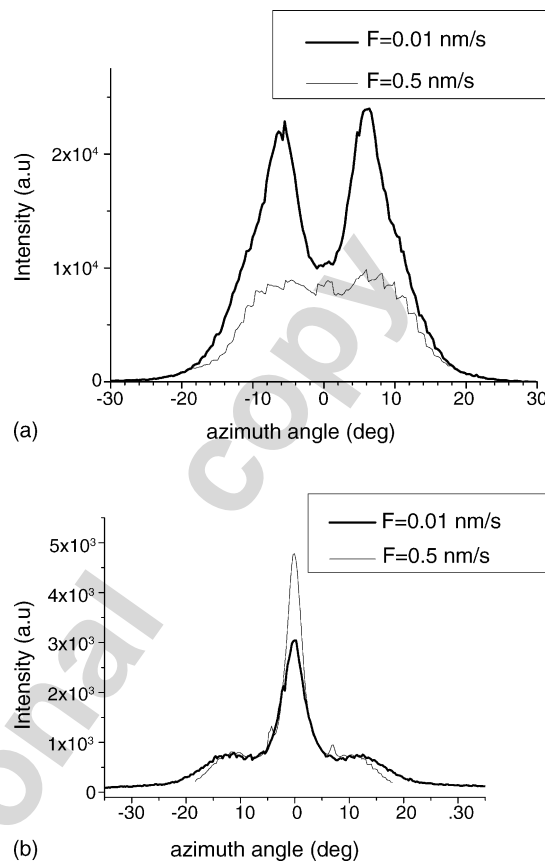
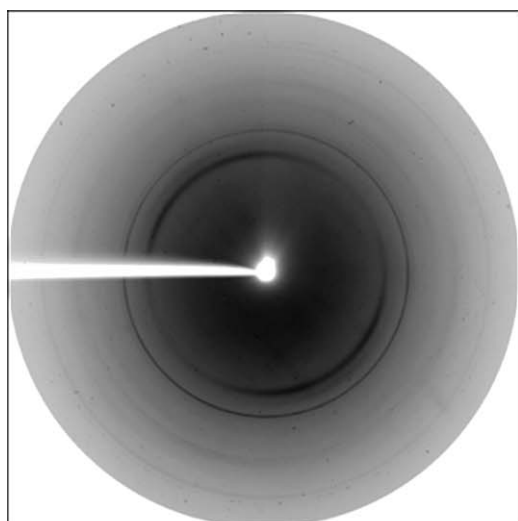


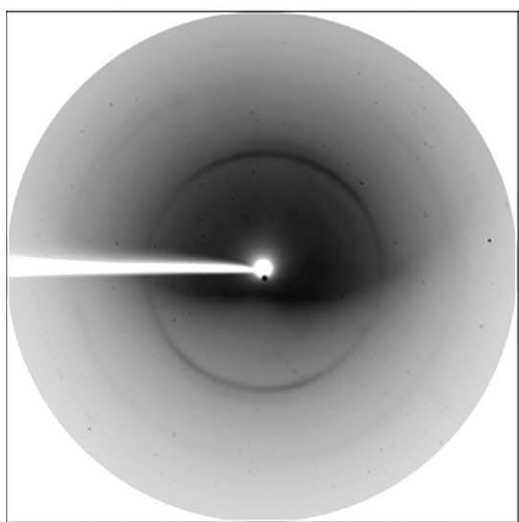
Fig. 5. Azimuth profiles along the 001 reflections for tetracene films grown at $F = 0.01$ and 0.5 nm/s on Mylar (a) and on SiO_2 (b).

poor charge transport properties. The lack of dependence of the FET mobility on the deposition flux for devices on Mylar can be explained by detrimental factors such as the disappearance of the preferential orientation of the crystallites and the atomic disorder balanced by beneficial ones such as the increase of the texturing, the decrease of the misorientation and the increase of the β thin film phase with the increase of the flux. Further investigations are needed to establish the correlation between charge transport and structural properties for films on Mylar. The investigation would have to take into account also morphological properties of the films since they play a primary role in determining the transport properties of the films [12].

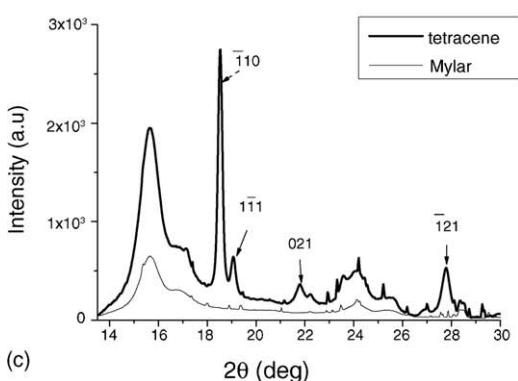
Thanks to the low X-ray absorption of Mylar, we could perform measurements also in transmission geometry. Fig. 6a shows the image diffracted by the tetracene film grown at $F = 0.01$ nm/s. It does not appreciably differ from that diffracted by the film deposited at the higher flux (not reported here). The nearly homogeneous intensity distribution along the Debye rings of the film, overlapped to the much broader ones produced by Mylar (Fig. 6b) confirms that the lattice planes responsible for them are almost randomly oriented with respect to the surface normal. In transmission geometry, the (hkl) planes of the crystallites fulfill the Bragg condition only if they are tilted with respect to the surface by μ such that $\mu = \theta_{hkl} + 90^\circ - \phi_{hkl}$, where ϕ_{hkl} is the angle between the plane and the surface and



(a)



(b)



(c)

Fig. 6. Diffraction images recorded in transmission geometry for: 50 nm-thick tetracene film grown at $F = 0.01$ nm/s on Mylar (a); pristine Mylar substrate (b). Intensity of the diffraction images integrated over the Debye rings on all the 2D detector area (c).

θ_{hkl} is the Bragg angle. In our case, only the hkl reflections with $\mu \leq 30^\circ$ are observed (they are better visible in the integrated pattern reported in Fig. 6c). This value indicates the upper limit of the tetracene crystallite misalignment.

4. Conclusions

Tetracene films grown by vacuum sublimation on Mylar substrates are formed by crystalline domains oriented with the $(00l)$ planes almost parallel to the surface but completely misoriented around the surface normal. Two polymorphs constitute the films namely, α and β thin film phases, that exhibit different $(00l)$ interplanar spacing corresponding to different molecular orientations. The amount of the α thin film phase, which has a structure closer to that of the bulk, decreases with decreasing deposition flux. Compared to films grown on SiO_2 , films on Mylar present a higher degree of crystallite misorientation and a larger static atomic disorder in the (hkl) lattice planes, which lead to a decrease in hole FET mobility for tetracene films grown on Mylar as compared to films on SiO_2 . In the future we will extend the investigation to different organic active materials and substrates to contribute to the understanding of general rules governing charge transport in organic thin films.

Acknowledgments

We would like to thank Marco Servidori (CNR-IMM) for his careful advice on the analysis of the data. We are also grateful to Prof. A. Bonfiglio (University of Cagliari, INFM-S3) for the substrate and to R. Zamboni (CNR-ISMN) for a stimulating discussion. Finally, we wish to thank the XRD1 beamline staff (Elettra) for the support provided during the measurements.

References

- [1] F. Garnier, G. Horowitz, X. Peng, D. Fichou, *Adv. Mater.* 2 (1990) 592.
- [2] G.H. Gelink, T.C.T. Genus, D.M. de Leeuw, *Appl. Phys. Lett.* 77 (2000) 1487.
- [3] J.A. Rogers, Z. Bao, K. Baldwin, A. Dodabalapur, B. Crone, V.R. Raju, V. Kuck, H. Katz, K. Amundson, J. Ewing, P. Drzaic, *Proc. Natl. Acad. Sci. U.S.A.* 98 (2001) 4835.
- [4] Y. Kato, S. Iba, R. Teramoto, T. Sekitani, T. Someya, H. Kawaguchi, T. Sakurai, *Appl. Phys. Lett.* 84 (2004) 3789.
- [5] C.W. Tang, S.A. Van Slyke, *Appl. Phys. Lett.* 51 (1987) 913.
- [6] J.H. Burroughes, D.D.C. Bradley, A.R. Brown, R.N. Marks, K. Mackay, R.H. Friend, P.L. Burns, A.B. Holmes, *Nature* 347 (1990) 539.
- [7] N.S. Sariciftci, L. Smilowitz, A.J. Heeger, F. Wudl, *Science* 258 (1992) 1474.
- [8] S.R. Forrest, *Nature (London)* 428 (2004) 911.
- [9] A. Hepp, H. Heil, W. Weise, M. Ahles, R. Schmechel, H. von Seggern, *Phys. Rev. Lett.* 91 (2003) 157406.
- [10] C. Santato, I. Manunza, A. Bonfiglio, F. Cicoira, P. Coseddu, R. Zamboni, M. Muccini, *Appl. Phys. Lett.* 86 (2005) 141106.
- [11] C. Santato, R. Capelli, M.A. Loi, M. Murgia, F. Cicoira, V.A.L. Roy, P. Stallinga, R. Zamboni, C. Rost, S.F. Karg, M. Muccini, *Synth. Met.* 146 (2004) 329.
- [12] F. Cicoira, C. Santato, F. Dinelli, M. Murgia, M.A. Loi, F. Biscarini, R. Zamboni, P. Heremans, M. Muccini, *Adv. Funct. Mater.* 15 (2005) 375.
- [13] F. Dinelli, M. Murgia, P. Levy, M. Cavallini, F. Biscarini, D.M. De Leeuw, *Phys. Rev. Lett.* 92 (2004) 116802.
- [14] G. Malliaras, R. Friend, *Phys. Today* 58 (2005) 53.
- [15] P. Syed Abthagir, Y.-G. Ha, E.-A. You, S.-H. Jeong, H.-S. Seo, J.-H. Choi, *J. Phys. Chem. B* 109 (2005) 23918.

- [16] R. Ruiz, A.C. Mayer, G.G. Malliaras, B. Nickel, G. Scoles, A. Kazimirov, H. Kim, R.L. Headrick, Z. Islam, *Appl. Phys. Lett.* 85 (2004) 4926.
- [17] A. Bonfiglio, F. Mamei, O. Sanna, *Appl. Phys. Lett.* 82 (2002) 3550.
- [18] W. Kraus, G. Nolze, *J. Appl. Cryst.* 29 (1996) 301.
- [19] D. Holmes, S. Kumaraswamy, A.J. Matzger, K.P.C. Vollhardt, *Chem. Eur. J.* 5 (1999) 3399.
- [20] S. Milita, M. Servidori, F. Cicoira, C. Santato, A. Pifferi, *Nucl. Instrum. Methods B* 246 (2006) 101.
- [21] A. Taylor, *X-ray Metallography*, John Wiley & Sons, 1961.
- [22] G. Witte, C. Woll, *J. Mater. Res.* 19 (2004) 1894.
- [23] C.D. Dimitrakopoulos, A.R. Brown, A. Pomp, *J. Appl. Phys.* 80 (1996) 2501.

Author's personal copy